

Study of Nonlinear Optical Responses of Phytochemicals of *Clitoria ternatea* by Quantum Mechanical Approach and Investigation of their anti-Alzheimer activity with In-Silico Approach

Shradha Lakhera

Uttarakhand Open University

Kamal Devlal

Uttarakhand Open University

Meenakshi Rana (✉ mrana@uou.ac.in)

Uttarakhand Open University

Ismail Celik

Erciyes University: Erciyes Universitesi

Research Article

Keywords: *Clitoria ternatea*, Clitorin, Dipole moment, Polarizability, Molecular Docking, MD Simulation

Posted Date: May 10th, 2022

DOI: <https://doi.org/10.21203/rs.3.rs-1535825/v1>

License: © ⓘ This work is licensed under a Creative Commons Attribution 4.0 International License.

[Read Full License](#)

**Study of Nonlinear Optical Responses of Phytochemicals of *Clitoria ternatea* by
Quantum Mechanical Approach and Investigation of their anti-Alzheimer activity with
In-Silico Approach**

Shradha Lakhera¹, Kamal Devlal¹, Meenakshi Rana^{1*}, Ismail Celik²

¹Department of Physics, School of Sciences, Uttarakhand Open University,
Haldwani, 263139, Uttarakhand, India

²Department of Pharmaceutical Chemistry, Faculty of Pharmacy, Erciyes University, Kayseri
38039, Turkey

Abstract

Clitoria ternatea is a flowering plant with promising medicinal plants with a wide variety of active phytochemicals. The present study aimed at the computational investigation of the nonlinear optical (NLO) responses of the active phytochemicals of the *Clitoria ternatea*. The computational investigation of the NLO features was done by using the density functional theory (DFT) by B3LYP/6-311G ++ (d, p) basis set. The structural parameters, mulliken charge distribution, and molecular electrostatic potential (MEP) surface clearly show the intramolecular charge transfer within Clitorin. The NLO properties were identified by computing the polarizability parameters. As the plant has high medicinal characteristics, the inhibiting properties of its phytochemicals were also investigated to combat Alzheimer disease (AD). The systematic *in-silico* study identifies Clitorin as the most active and inhibiting phytochemicals of the plant. The results obtained from molecular dynamics (MD) simulation tell the stability of the complex and make it a fair selection as a drug-like molecule against AD. The cardio-toxicity analysis done for the Clitorin molecule verifies that it is harmless for the heart.

Keywords: *Clitoria ternatea*; Clitorin; Dipole moment; Polarizability; Molecular Docking, MD Simulation

*Corresponding author: E-mail: mrana@uou.ac.in

1. Introduction

The research-based on naturally existing compounds has occupied a vast part in the development of science and technology [1]. Pharmaceuticals, medicinal sciences, cosmetics, infrastructure development, health supplements, luminescent materials, cleansing agents, synthetic fibres, dyes, coatings, lasers, microfabrication, etc., are the major fields of research where naturally existing compounds has made a significant volume [2]. The reason behind their wider applications than the human made compounds is their high reactivity, non-hazardous and better efficiency. Due to having high reactivity, the natural compounds have many interdisciplinary applications also. Even in multimedia science, data storage, sensing devices, non-linear optical (NLO) devices these compounds have grown up their applications [3]. Therefore, the development of new organic NLO materials has given birth to the new era of material science and engineering. The literature survey had shown that faster response time, higher thermal stability, better optical frequency transform, and stronger intramolecular charge transfer are observed in the organic NLO materials like L-arginine maleate dihydrate, L-methionine L-methioninium hydrogen maleate, Urea, etc [4-5]. Thus, the development of organic NLO supplements is a more convenient and followed area of research among the researchers. Numerous studies depending on the development of NLO materials from plant phytocompounds have been recorded so far. The investigation of the NLO behavior of the esterified derivative of Brassicasterol by computational approaches [6] had been reported. Some of the studies of the development of NLO candidates from plant derivatives are from *Alpinia calcarata* silver nanoparticles [7], *Dioscorea alata* [8], *Mirabilis jalapa* [9], *coriandrum sativum* extracts [10], chlorophyll-*a* extracted from *Andrographis paniculata* leaves [11], curcumin derivatives [12], etc.

Clitoria ternatea, a perennial flowering plant is one of the most used medicinal plants (Figure 1) like antioxidant, hypolipidemic, anticancer, anti-inflammatory, analgesic, antipyretic, antidiabetic, antimicrobial, gastro-intestinal antiparasitic, etc [13,14]. It is known by different names as Asian pigeonwings, blue bell vine, blue pea, butterfly pea, cordofan pea, Darwin pea, and many more. Leaves, roots, flowers, seeds, and even roots of this plant are beneficial. The numerous biological activities of its phytochemicals make it significant for research. The high reactivity of the phytochemicals can be interpreted as high polarizabilities. Thus, its phytochemicals can also be considered for the development of organic NLO materials. Its major phytochemicals include Cinnamic acid, Delphinidin-3,5-diglucoside, Flavanol 3-O-D-glucoside, Genistein, Kaempferol, Kaempferol-3,7-diglucoside, Clitorin, Linolenic acid, Oleic

acid, Palmitic acid, Taraxerol, and Taxaxeron [15,16]. These phytochemicals are seen to be mentioned in most of the studies done with this plant.

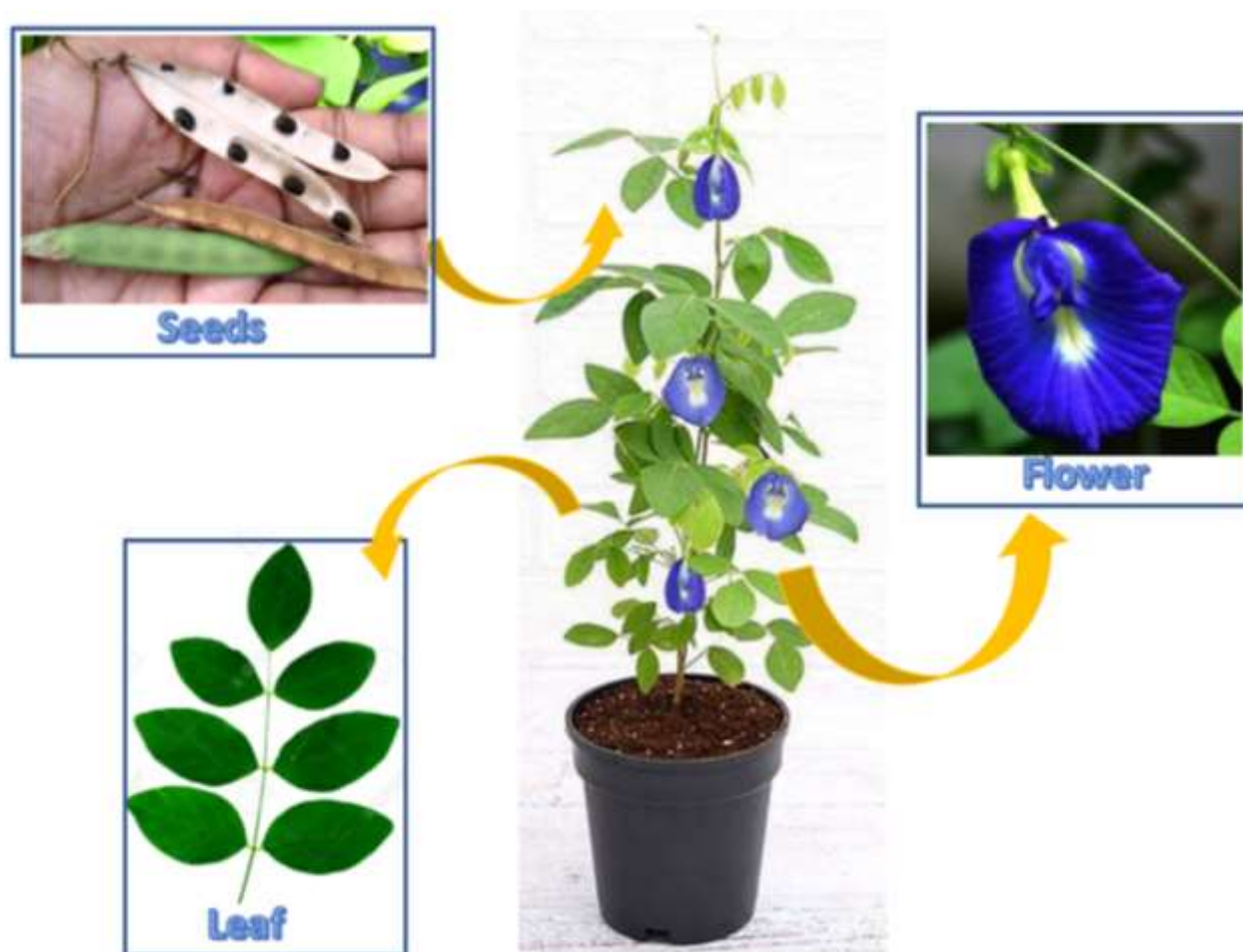


Figure 1. Morphology of *Clitoria ternatea* plant.

Since *Clitoria ternatea* has many active phytochemicals and medicinal property, therefore, in the present study we have investigated the NLO properties of the phytochemicals of the *Clitoria ternatea* plant. The computational study was performed with the phytochemicals of this plant using density functional theory (DFT). The optimization of the structures of the phytochemicals was done that reveals the quantum chemical properties of the phytochemicals. The initial screening of the reactive molecule was done by dipole moment and the molecule with the highest dipole moment was selected for the further inquiry of NLO behavior. The detection of NLO activity of the selected molecule was further done by performing reactivity analysis, spectral analysis, and calculating polarizability parameters.

Promoting the interdisciplinary side of this study, a systematic *in-silico* study was also performed with the active phytochemicals of *Clitoria ternatea*. The *in-silico* modeling is

generally used computer-aided drug designing (CADD) technique that is preferred by the chemists and researchers for the evaluation of the drug-like character of the selected systems. Thousands of research works had been reported based on CADD like *Feverfew* and *Piper longum* was used against the M^{pro} and PL^{pro} of COVID-19 [17,18], *Tridax procumbens* was used against MCM7 breast cancer [19], *Blumea mollis* was used as anti-fungal candidate[20], *Bjerkandera adusta* used against Proteostasis Network Modules [21], *Curcuma longa* (Turmeric) and *Cymbopogon citratus* (lemon grass) as lipoxygenase inhibitor [22] and many more. Thus, motivated by this fact, *in-silico* modeling of selected most active phytochemicals of the *Clitoria ternatea* plant had also been performed in this study. Many studies were seen reporting the pharmacological uses of *Clitoria Ternatea* derivatives in treating neurological disorders. A review of the neuropharmacological potentiality of Clitorin is explained in detail in the cited paper [23,24]. It is also used as an anti-oxidant [25]. It is also used as a base supplement for eye drop [26]. Apart of this, this plant is also used for the treatment of various brain diseases like dementia, depression, brain cancer (cell cycle checkpoint proteins in the cyclin/CDK pathway in cancer cells), and many more [27,28]. Thus, it can be said that the derivatives of the title plant can be used for medicating the brain or neuro-related sickness. Keeping this in mind, the phytochemicals of the title plant are used for inhibiting the BACE1 macromolecule of Alzheimer disease (AD). AD is a neurodegenerative disease that is mostly found in people over 65 years of age. Molecular docking was performed to check the extent of the binding of ligands at the reactive binding sites of the target macromolecule. Cardio-toxicity was also determined for the ligand having the best binding score. Molecular Dynamics (MD) simulation was performed targeting a novel clinical candidate BACE1 receptor for the treatment of AD.

2. Computational Procedure and Calculation

2.1. Chemical reactivity and NLO activity

The PDB structures of fourteen phytochemicals of the *Clitoria ternatea* were downloaded from the online database “IMPPAT (Indian Medicinal Plants, Phytochemistry, And Therapeutics)” (<https://cb.imsc.res.in/imppat/home>) and their structures with chemical formulae are mentioned in SD 1. The software “Open Babel” (http://openbabel.org/wiki/Main_Page) was used to convert the PDB files into gif files. In order to investigate the NLO responses of the phytochemicals, the structures of the phytochemicals were optimized using the software Gaussian 09 [29] (<https://gaussian.com/glossary/g09/>). The results were analysed using the GUI “GaussView 5.0” [30] (<https://gaussian.com/gaussview6/>). All the computational

calculations were done for the ground state of the structures using DFT with Becke-3-Lee-Yang-Parr (B3) exchange function combined with (LYP) correlation and 6-311G basis set [31]. The optimized geometries were used for the further detection of stability and chemical reactivity checks. The energy corresponding to the frontier molecular orbitals (FMO) was also derived from the optimized geometries which were used for the calculations of global reactivity parameters. These parameters are calculated with the help of Koopman's equations [32] given below:

$$\Delta E = E_{LUMO} - E_{HOMO} \dots\dots\dots (1)$$

$$IP = -E_{HOMO} \dots\dots\dots (2)$$

$$EA = -E_{LUMO}, \dots\dots\dots (3)$$

$$CP = \frac{E_{HOMO} + E_{LUMO}}{2}, \dots\dots\dots (4)$$

$$\chi = \frac{(IP + EA)}{2}, \dots\dots\dots (5)$$

$$\eta = \frac{E_{LUMO} - E_{HOMO}}{2}, \quad S = \frac{1}{\eta}, \dots\dots\dots (6)$$

The electronic spectra were computed using TD-DFT (Time Dependent-DFT) method. The vibrational spectra were also computed using the same basis set. In Raman spectra analysis, Raman intensity is also calculated corresponding to high frequency modes. It was calculated by below given expression:

$$I = \frac{f(v_0 - v_i)^4 S_i}{v_i \left[1 - \exp\left(-\frac{hc v_i}{kT}\right) \right]} \dots\dots\dots (7)$$

where I refer to Raman intensity of the considered mode, f is a constant with value 10^{-12} , v_0 has value 9398.5 cm^{-1} . v_i and S_i is the vibrational wavenumber and Raman activity of selected mode respectively. h , c , k , and T have their usual meanings. The UV-Vis and the Raman spectra was plotted using software "Origin 2021" (<https://www.originlab.com/>). For NLO analysis, the polarizability parameters total dipole moment (μ_{total}), total isotropic polarizability (α_{total}), anisotropy of polarizability ($\Delta\alpha$), and first order hyperpolarizability (β_{total}) were calculated by the following given formulae:

$$\mu_{tot} = (\mu_x^2 + \mu_y^2 + \mu_z^2)^{\frac{1}{2}} \dots\dots\dots (8)$$

$$\alpha_{tot} = \frac{1}{3}(\alpha_{xx} + \alpha_{yy} + \alpha_{zz}) \dots\dots\dots (9)$$

$$\Delta\alpha = \frac{1}{\sqrt{2}} [(\alpha_{xx} - \alpha_{yy})^2 + (\alpha_{yy} - \alpha_{zz})^2 + (\alpha_{zz} - \alpha_{xx})^2 + 6\alpha_{xz}^2 + 6\alpha_{xy}^2 + 6\alpha_{yz}^2]^{\frac{1}{2}} \dots\dots\dots (10)$$

$$\langle\beta\rangle = [(\beta_{xxx} + \beta_{xyy} + \beta_{xzz})^2 + (\beta_{yyy} + \beta_{yzz} + \beta_{yxx})^2 + (\beta_{zzz} + \beta_{zxx} + \beta_{zyy})^2]^{\frac{1}{2}} \dots\dots\dots (11)$$

where μ_x , μ_y , and μ_z are the tensor components dipole moment, α_{xx} , α_{yy} , and, α_{zz} are the tensor components of polarizability and β_{xxx} , β_{yyy} , and β_{zzz} are the tensor components of hyperpolarizability.

2.2. Investigation of pharmacological activity

The *in-silico* study was performed for the detection of the anti-Alzheimer activity of the phytochemicals of the *Clitoria ternatea*. The structure of the candidate β -Site amyloid precursor protein cleaving enzyme 1 (BACE1) inhibitor (PDB ID: 4B05) was selected as the target macromolecule and was downloaded from the online database Protein Data Bank (<https://www.rcsb.org/>). The BACE1 is known to produce the toxic amyloid β (A β) that leads to the early evolution of pathogens of AD in the human body [33]. Thus, the prevention from BACE1 will be worthwhile in blocking the development of pathogens of AD in the body. This became the major reason in considering BACE1 is a target macromolecule. The crystal structure of the BACE1 target macromolecule developed with X-ray crystallography having resolution 1.80 Å is shown in Figure 2.

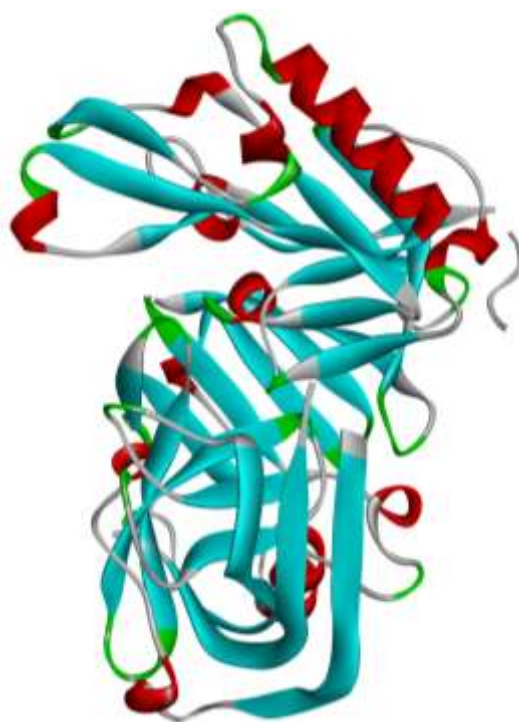


Figure 2. Crystal structure of BACE1 inhibitor (PDB ID: 4B05).

Molecular docking was done for the selection of the phytochemical having the best binding with the target macromolecule. This will help in selecting the ligand which will have the best inhibition tendency against the AD. The software “AutoDock Vina” (<https://vina.scripps.edu/>) was used for performing docking. The algorithm for docking was followed by the energy difference of 4 kcal/mol and grid box centred at $(x, y, z) = (-2.273, 1.428, -15.310)$. Docking results were analysed by the software “Biovia Discovery Studio Visualizer” (<https://discover.3ds.com/discovery-studio-visualizer-download>). The best pose of the ligand having best binding affinity was selected on the basis of the highest number of hydrogen bonds. Cardio-toxicity was also predicted for the molecule having the best binding affinity to check whether the drug-like molecule will create any cardio-related harm to the body after consumption. The cardio-toxicity was investigated by using Pred-hERG 4.2 webserver (<http://predherg.labmol.com.br/>) [34]. The canonical smileys were used for the prediction of the probability map of the compound. For compounds to be non-cardio-toxic, the confidence value should not exceed 0.26. Different fragments like potency, confidence, applicability domains are given by the cardio-toxicity analysis.

MD simulation was further be computed for protein-ligand complex having the best binding score. The MD simulation will be performed using software “Gromacs 2019.2 version”. The

protein macromolecule was prepared using pdb2gmx with Gromos96 54a7 force field, and ligand topology was formed the GlycoBioChem PRODRG2 Server. The complex was simulated for 100 ns in canonical (amount of substance (N), pressure (P) and temperature (T) – NPT) and Isothermal-isobaric (amount of substance (N), volume (V), and equilibrium steps temperature (T) – NVT) ensembles. The parameters like Root mean square deviation (RMSD) and Root mean square fluctuation (RMSF), binding energy, hydrogen bond, and radius of gyration (Rg) [35,36].

3. Results and Discussion

3.1. Structure and charge analysis

The structure of phytochemicals Cinnamic acid, Clitorin, Delphindin-3,5-diglucoside, Flavonol 3-O-D-glucoside, Genistein, Kaempferol, Kaempferol-3,7-diglucoside, Linolenic acid, Oleic acid, Palmitic acid, Taraxerol, and Taxaxeron were optimized using DFT (SD 1). The net polarity of the molecules was obtained by optimized geometries of the structures. The values of dipole moment obtained from the optimized geometries are mentioned in SD 2. Clitorin has dipole moment of 10.28 Debye that is highest among all other considered phytochemicals Cinnamic acid (2.68 Debye), Kaempferol-3,7-diglucoside (6.41 Debye), Flavanol 3-O-D-glucoside (2.17 Debye), Genistein (5.32 Debye), Kaempferol (6.15 Debye), Linolenic acid (1.74 Debye), Oleic acid (4.64 Debye), Taraxerol (1.69 Debye), and Taxaxeron (3.35 Debye). The high value of dipole moment is due to high value of intramolecular interactions and these interactions may leads to high polarizability [37]. The difference between the dipole moment of Clitorin and other molecules seem to be high enough to do fair selection of Clitorin for the NLO investigation. Based on this, Clitorin was taken into consideration for the further computational and spectral study. The optimized structure of Clitorin molecule is shown in Figure 3. The Clitorin molecule is a large molecule with 92 atoms associated to it. The structural stability of Clitorin molecule was studied by analysing bond lengths and bond angles of the molecule. The structural parameters are mentioned in the SD 3 and SD 4. The total energy of Clitorin is found -1700895.541 kcal/mol. Higher magnitude of bond length was observed for the C – C bonds throughout the geometry. On the other hand, the O – H bonds of the geometry have comparatively lower magnitudes of the bond lengths that can be easily dissociated. This shows the possibility of the dislocation of free electron pairs from the –OH groups towards the C – C bonds of the benzene ring. Similar possibility of the charge dislocation can be seen by the bond angles. The angles corresponding the C – C – C are higher than the angles corresponding to the C – H – O angles. The mulliken charge distribution was

also analyzed for the Clitorin molecule and are mentioned in SD 5. The oxygen atoms contribute to the negative charge and the hydrogen atoms contribute in the making of the positive charge of the molecule. However, the simultaneous positive and negative charge contribution of the carbon atoms is observed for the Clitorin molecule. The –OH groups act as the electron-donating parts of the molecule and the free electron charge cloud gets dislocated towards the aromatic benzene rings.

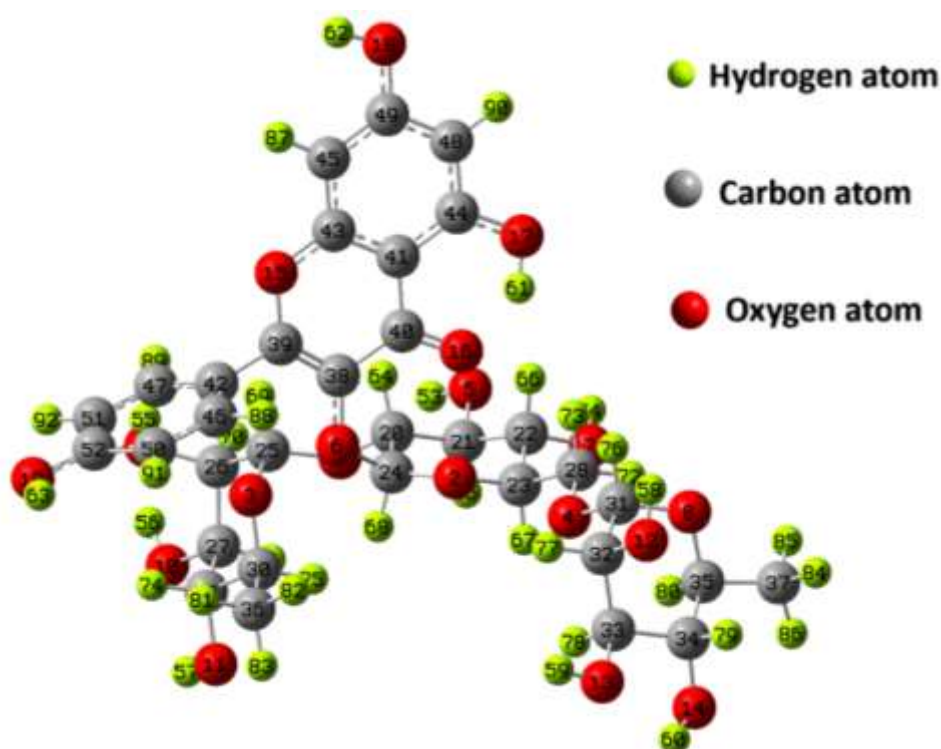


Figure 3. Optimized geometry of Clitorin molecule obtained using B3LYP/6-311G (++, p) basis set.

3.2. Molecular electrostatic potential (MEP) and frontier molecular orbital (FMO) analysis

The MEP surface of the Clitorin molecule is illustrated in Figure 4. MEP surface of the molecule indicates the nucleophilic (blue) region and the electrophilic (red) region. The existence of these regions indicates the possibility of intramolecular charge transfer (ICT). The nucleophilic regions of the MEP are majorly induced by –OH groups and the electrophilic regions are located over the C – C bonds and C = C bonds of the benzene rings. Thus, the ICT is taking place throughout the molecule's geometry despite transferring from functional groups. The MEP surface is shown in Figure 4(a) shows the nucleophilic regions and Figure 4(b) shows electrophilic regions.

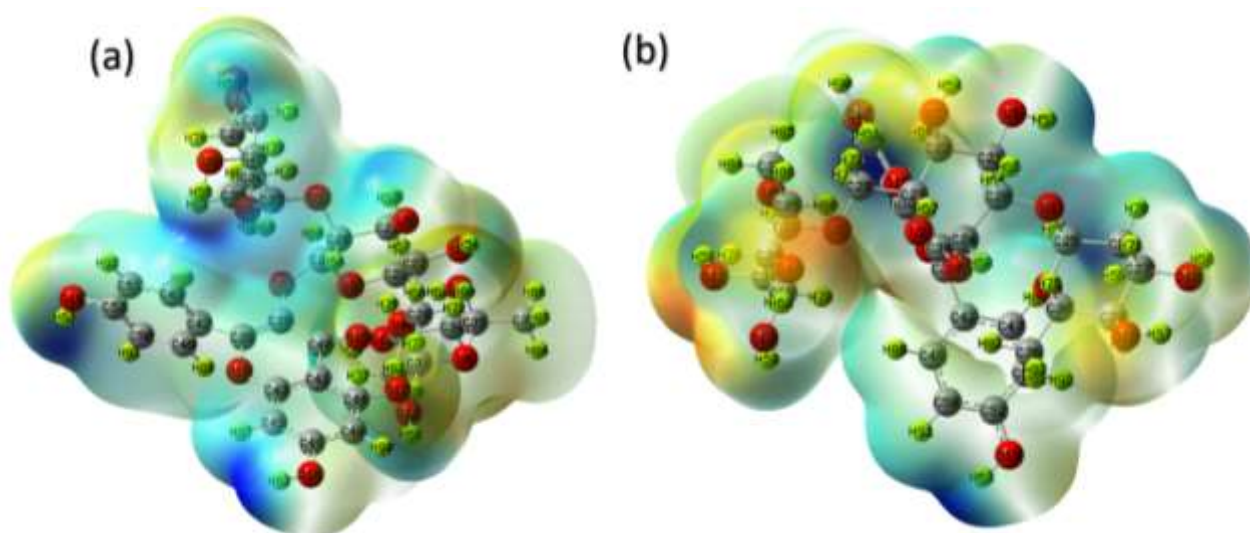


Figure 4. Molecular electrostatic potential (MEP) surface of the Clitorin molecule showing electrophilic and nucleophilic region.

The FMO is used to establish the stability and the chemical reactivity of Clitorin. These parameters are considered as the frontier of the electrons and are mentioned in SD 6. The energy corresponding to the highest occupied and lowest unoccupied molecular orbitals (HOMO-LUMO energies) was derived from the optimization. The molecular orbital surfaces were also computed for the Clitorin molecule and the molecular orbital surfaces are illustrated in Figure 5. The molecular orbital surfaces are distributed only on the benzene ring made from atoms sequencing from 38C to 49C. However, there is not any major change in the distribution of HOMO-LUMO surfaces. The value of ΔE for Clitorin was computed as 4.343eV. The value of ΔE for Clitorin is found to be less than the ΔE of the NLO reference materials Urea (7.43 eV) and Potassium dihydrogen phosphate (KDP) (6.835 eV). The moderate value of ΔE shows high excitation of electrons that shows the molecule is reactive. The high value of IP (6.597 eV) was reported for the Clitorin that shows the free electron releasing tendency of the Clitorin electron donating part. Low value of EA i.e., 2.254 eV was obtained that shows the electron accepting part of the Clitorin molecule will not face and will easily attract the electron cloud. The low value of CP (-4.425eV) and high value of χ (4.425 eV) for Clitorin shows the high stability of the molecule. The chemical hardness (2.171 eV) for the Clitorin molecule was recorded as positive. This shows the Clitorin molecule stay stiff and rigid. All the computed parameters show that the Clitorin molecule is chemically reactive in nature.

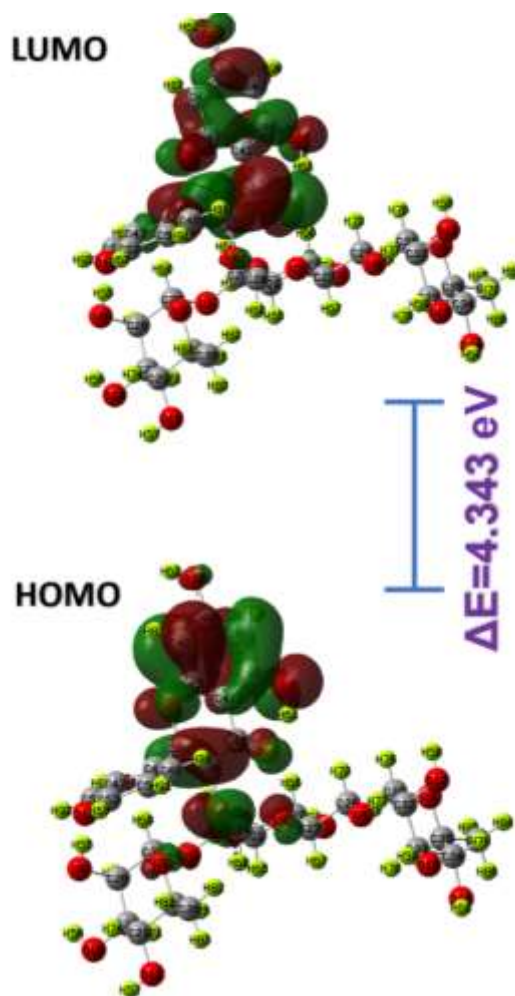


Figure 5. Molecular orbital surface distribution of Clitorin molecule with computed energy gap.

3.3. Vibrational spectra analysis

As the polarizing ability of any compound is proportional to the Raman intensity [38]. The Raman modes with high intensity are illustrated in Figure 6. The details of the high intensity modes are mentioned in SD 7. The torsional bending (δ) of the C – H bonds are observed from 800 to 1300 cm^{-1} . The mode δ_{CH} at 855.17 cm^{-1} frequency has the highest value of Raman intensity 1808.13 cm^{-1} . The mode ν_{CC} with high intensity 5412.76 cm^{-1} is observed with frequency 1679.64 cm^{-1} . The C – O bonds stretches linearly and the mode with highest intensity of 3798.18 cm^{-1} is observed with frequency 1771.92 cm^{-1} . The asymmetric stretching (α_{CH}) of C – H bonds are observed around 2978-3149 cm^{-1} . The α_{CH} with frequency 2991.83 cm^{-1} has the highest Raman intensity (1037.4 cm^{-1}). The symmetric stretching (ν_{CH}) for C – H bonds have highest mode with intensity 1209.95 cm^{-1} . The computed values of Raman intensity are extremely high. These high values are due to the presence of conjugated- π electrons of C – C

bonds. The high values of Raman intensity give rise to the high value of polarizability in Clitorin molecule.

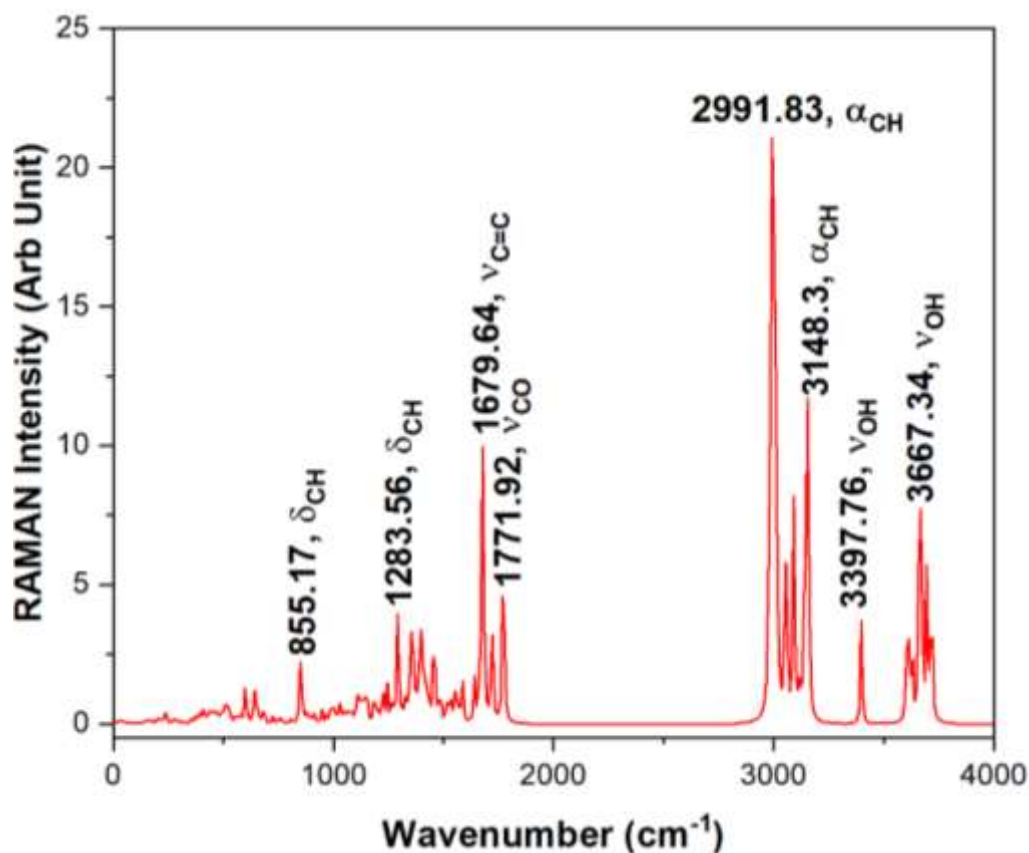


Figure 6. Computed Raman spectra of Clitorin molecule. (Vibrational modes: ν -symmetric stretching, α -asymmetric stretching, δ -torsional bending.)

3.4. Absorption spectra analysis

The electronic spectra were computed by performing energy optimization of the Clitorin molecule by the TD-DFT method. UV-Vis spectra of Clitorin is illustrated in Figure 7 and the transition details are mentioned in SD 8. The transition $S_0 \rightarrow S_1$ at 341.82 nm wavelength and 3.62 eV excitation energy majorly imparts in the formation of the broad absorption band of Clitorin molecule. These transitions are induced by the presence of $\pi \rightarrow \pi^*$ and $n \rightarrow \pi^*$ bonds as these bonds produce strong absorption peaks around 300-400 nm and absorption boundary at 450-460 nm. The transitions $S_0 \rightarrow S_2$ and $S_0 \rightarrow S_3$ that leads to the absorption spectra are at wavelengths 327.83, and 299.42 nm with excitation energies 3.78 eV, and 4.74 eV respectively. Thus, the high excitation energies of these transitions show the high chemical reactivity of the Clitorin molecule. It also leads to the high binding ability of the ligand to the active binding sites of the macromolecule [39].

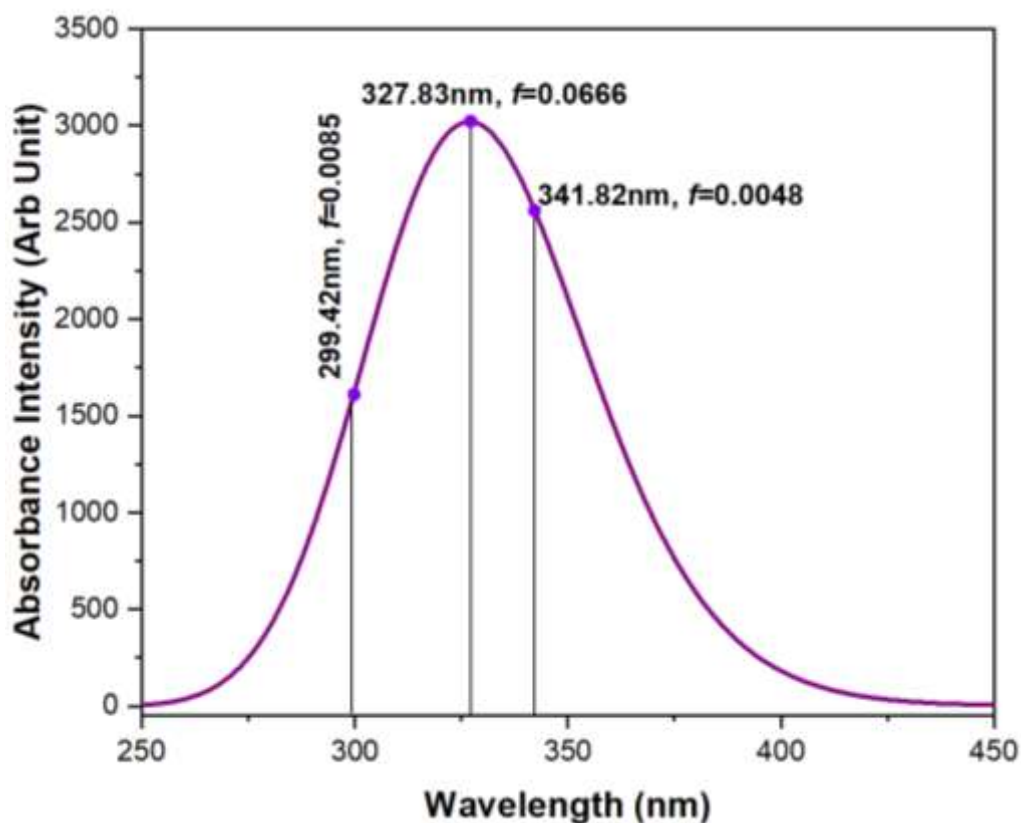


Figure 7. Computed UV-Vis absorption data of Clitorin molecule.

3.5. Nonlinear optical analysis

The molecular packing, intramolecular and intermolecular interactions has straight association with the physicochemical properties of the molecules [40]. Thus, the quantum chemical calculations were carried out to predict the nature of electric dipole moment (μ_{total}), polarizability (α_{total}) and first order hyperpolarizability (β_{total}). The tensor components of μ_{total} , $\Delta\alpha$ and β_{total} were computed by polar calculations and are mentioned in Table 1. The value of μ_{total} for Clitorin was computed as 4.046 Debye. The comparison gave us that the μ_{total} for Clitorin was 2.5 times than that of most generally used reference NLO material, Urea (1.527 Debye). Highly raised values of α_{total} (62.514×10^{-24} esu) and $\Delta\alpha$ (111.87×10^{-24} esu) for Clitorin are reported. α_{total} of Clitorin was obtained 11 times higher than Urea (5.664×10^{-24} esu) and $\Delta\alpha$ was nearly 18 times to that of Urea (6.304×10^{-24} esu). The value of β_{total} for Clitorin 5.415×10^{-30} esu was nearly 7 times higher than Urea (0.781×10^{-30} esu). For the validation of Clitorin being a good candidate as NLO material, the β_{total} for Clitorin was also compared with some already worked compounds that were experimentally proven NLO active materials and had been used in various applications in nonlinear optics. Such compounds were mentioned in Table 2. Compounds like 3-nitroaniline, Phenyl urea, thiosemicarbazone derivatives, thiourea-

glutaric acid, indole-7-carboxaldehyde, 2,4,6-triaminopyrimidine, and ANDIROBIN have low values of β_{total} than that of Clitorin. These values were quite less than that of Clitorin that validates the good candidature of Clitorin being nonlinearly active.

Table 1. Computed values of dipole moment, polarizability and first order hyperpolarizability of Clitorin (dipole moment in Debye and all tensor components are in a.u. and α_{total} , $\Delta\alpha$ and β_{total} in esu).

| Dipole moment | | | Polarizabilities | | | First order hyperpolarizability | | |
|---------------|----------|---------|------------------|--------------------------|-------------------------|---------------------------------|-------------------------|-------------------------|
| Component | Clitorin | Urea | Component | Clitorin | Urea | Component | Clitorin | Urea |
| μ_x | -3.35 | 1.28 | α_{xx} | 435.257 | 39.260 | β_{xxx} | -82.66 | 24.729 |
| μ_y | 2.082 | 0.00004 | α_{xy} | 3.553 | 24.690 | β_{xxy} | 300.061 | 0.006 |
| μ_z | 0.902 | -0.830 | α_{yy} | 433.886 | 38.219 | β_{yyy} | 210.531 | 32.896 |
| μ_{total} | 4.046 | 1.527 | α_{xz} | -51.058 | 0.2947 | β_{yyy} | -619.337 | 31.817 |
| | | | α_{yz} | -26.335 | -1.159 | β_{xxz} | -226.921 | -0.499 |
| | | | α_{zz} | 396.335 | 0.454 | β_{xyz} | -318.121 | -61.443 |
| | | | α_{total} | 62.514×10^{-24} | 5.664×10^{-24} | β_{yyz} | 46.292 | 19.374 |
| | | | $\Delta\alpha$ | 111.87×10^{-24} | 6.304×10^{-24} | β_{zzz} | 149.28 | 0.5057 |
| | | | | | | β_{yzz} | 271.026 | -20.593 |
| | | | | | | β_{zzz} | -379.504 | 0.225 |
| | | | | | | β_{total} | 5.415×10^{-30} | 0.781×10^{-30} |

Table 2. Some already known and experimentally proven NLO active materials with their hyperpolarizability values.

| Material | Hyperpolarizability | Reference |
|--|--------------------------|-----------|
| 3-nitroaniline | 1.347×10^{-30} | [41] |
| Phenyl Urea | 2.043×10^{-30} | [42] |
| (E/Z)-4-benzyl-1-(1-ferrocenylethyl)thiosemicarbazone | 2.1433×10^{-30} | [43] |
| (E/Z)-4-(4-chlorobenzyl)-1-(1-ferrocenyl-ethyl)thiosemicarbazone | 1.293×10^{-30} | [43] |
| (E/Z)-4-(2-bromo benzyl)-1-(1-ferrocenylethyl)thiosemicarbazone | 3.316×10^{-30} | [43] |
| thiourea-glutaric acid | 3.57×10^{-30} | [44] |

| | | |
|---|-------------------------|------|
| Indole-7-carboxaldehyde | 3.96×10^{-30} | [45] |
| 2,4,6-triaminopyrimidine | 4.73×10^{-30} | [46] |
| methyl-2{(1R,2R)-2-[(1aS, 4S, 4aS, 8aS)-4-(furan-3-yl)-4a-methyl-8-methylene-2-oxooctahydrooxireno[2,3-d]isochromen-7-yl]-2,6,6-trimethyl-5-oxocyclohex-3-en-1-yl}acetate (ANDIROBIN) | 3.759×10^{-30} | [47] |

3.6. *In-silico* study

3.6.1. Molecular docking analysis

Molecular docking was performed to check the binding ability of the considered ligands with BACE1 inhibitor (PDB ID: 4B05). The docking results were recorded after performing ten times docking with each and every ligand. The docking score of all the considered ligands is mentioned in SD 9. Clitorin, Delphinidin 3,5-diglucoside, Taraxerol and Taraxeron were the molecules that have the highest binding affinity of -10.4 kcal/mol, -10.2 kcal/mol, -10.7 kcal/mol, and -10.6 kcal/mol respectively. These binding scores are extremely higher than the other ligands Cinnamic acid (-5.8 kcal/mol), Genistein (-7.9 kcal/mol), Kaempferol (-7.9 kcal/mol), Kaempferol-3,7-diglucoside (-9.3 kcal/mol), Linolenic acid (-5.8 kcal/mol), Octadeca-9,12-dienoic acid (-4.9 kcal/mol), Oleic acid (-5.7 kcal/mol), and Palmitic acid (-4.8 kcal/mol). The validity of the docking scores was supported by analyzing the number of hydrogen bonds and the dipole moment of Clitorin, Delphinidin 3,5-diglucoside, Taraxerol, and Taraxeron. The details of the number of hydrogen and hydrophobic bonds and dipole moment of these ligands are mentioned in SD 10. The binding of ligand to the binding sites of the macromolecule is considered stable by the raised value of hydrogen bonds. As hydrogen bonds involve the availability of high electronegativity, they are the strongest bonds among the other known strong intermolecular bonds. Similarly, hydrophobic bonds are the strongest among the other known weak intermolecular bonds. Thus, the more the number of hydrogen and hydrophobic bonds associated with the binding site, the more will be the strength of binding. Clitorin thus has the highest number of 7 hydrogens and 6 hydrophobic bonds associated with the binding site. The dipole moment that is the virtue of the high polarity of the molecule is also highest for Clitorin. High polarity leads to high reactivity. Clitorin has a dipole moment equal to 3.62 Debye which is higher than Delphinidin 3,5-diglucoside (2.47 Debye), Taraxerol (1.76 Debye), and Taraxeron (3.48 Debye). Therefore, analysis of the docking score,

hydrogen bonds, hydrophobic bonds, and dipole moment suggests Clitorin as the most reactive and finely bonded ligand. The details of the hydrogen and hydrophobic bond interactions formed by binding of Clitorin with protein were shown in SD 11 and the 2D illustration of all the interactions is shown in Figure 8. The visual representation of docking results of the best pose of Clitorin bonded with target protein is shown in Figures 9(a) and 9(b). Thus, the protein-ligand complex obtained after docking was taken for MD simulation.

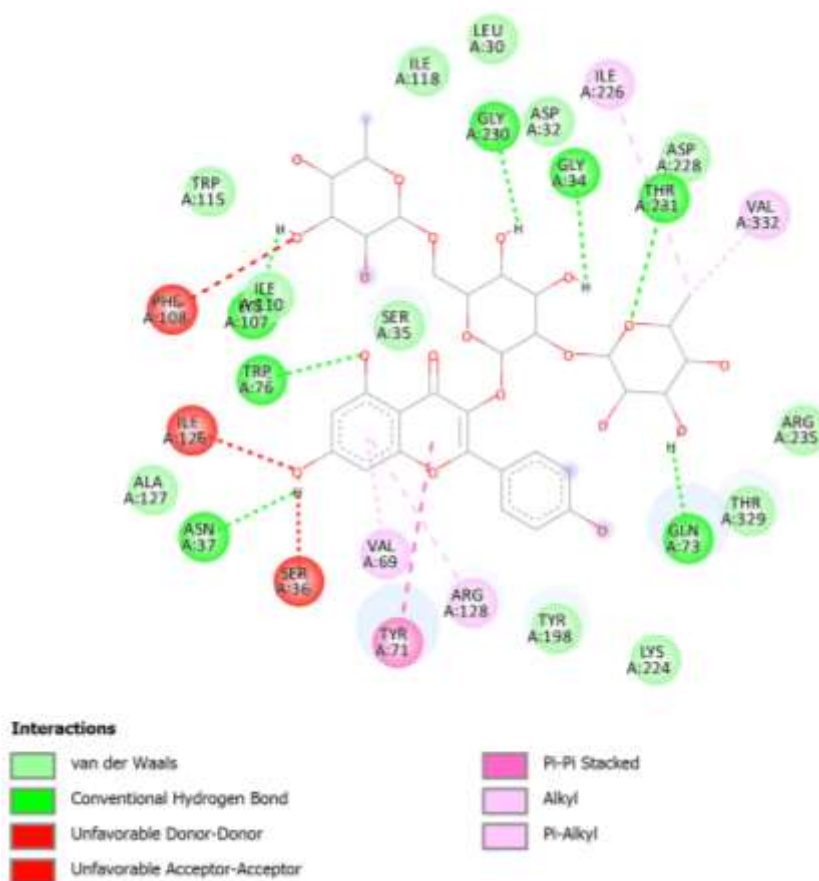


Figure 8. 2D view hydrogen bond interactions associated to protein-ligand complex after docking.

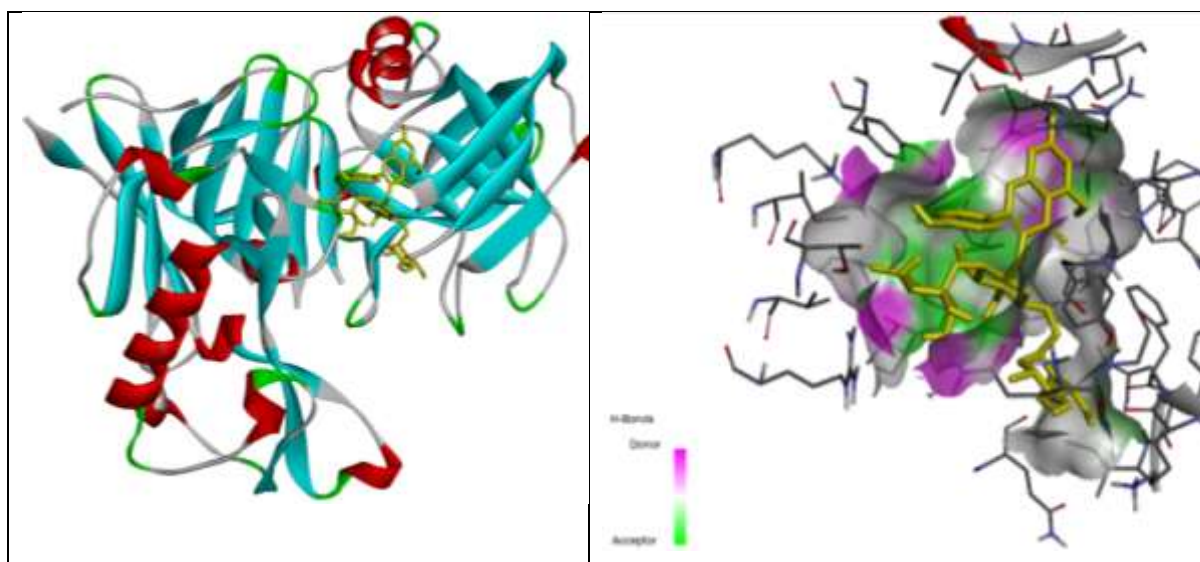


Figure 9. (a) Binding site of the protein where the ligand (yellow color) is attached. (b) 3D view of protein-ligand interaction within the surface due to H-bonds.

3.6.2. MD simulation analysis

The physical movements of the complex molecules were analyzed by MD Simulation. Cocrystal ligand AZD3839 is an experimental inhibitor of BACE1 that is often used for comparing the simulation results obtained from the simulation of the protein-ligand complex. The cocrystal ligand AZD3839 and protein complexed with ligand were simulated for 100 ns of time trajectory and the results are compared. This helps in obtaining dynamic data at atomic spatial resolution. The RMSD, RMSF, binding energy, hydrogen bond, and Rg were obtained as the results from simulation and the results are illustrated in Figure 10.

RMSD value of BACE1 with Clitorin and cocrystal ligand AZD3839 seems to fluctuate between 0.2 to 0.5 nm. The average value of the RMSD value of the complex is around 0.35 nm. The RMSD trajectory of the complex is slightly higher than the cocrystal ligand AZD3839. This variation is due to the position restraints. The energy minimization in structures results in these variations. The RMSF value of the complex shows a certain rise around residue 50, 180, and 300. However, the RMSF trajectory of BACE1 complexed with Clitorin and cocrystal ligand AZD3839 doesn't differ much. The average value of the RMSF of the complex is around 0.3 nm. The highest rise of the RMSF trajectory of the complex is 0.6 nm at 50 residue number. Thus, the RMSD and RMSF values of the complex show that the ligand binds strongly to the protein binding site and protein remains unaltered due to the presence of ligand. The RMSD and RMSF fluctuations are illustrated in Figures 10(a) and 10(b).

R_g shows the compactness of the protein-ligand complex. The trajectories of R_g of BACE1 complexed with Clitorin and cocrystal ligand AZD3839 have the variation that shows the stability of the complex. The R_g values of the complex are low than the values of the R_g of cocrystal ligand AZD3839. The complex value fluctuates between 2.1 to 2.2 nm during the simulation time. The trajectory reaches the highest peak of 2.2 nm five times at 37ns, 45ns, 76ns, 85ns, and finally rises after 85ns up to 2.25 nm. These fluctuations are less than that of cocrystal ligand AZD3839. The R_g fluctuations of both systems are illustrated in Figure 10(c). The lesser value of R_g denotes the compactness of the complex.

The hydrogen bond count imparts in stabilizing the complex. The hydrogen bond count of the complex fluctuates between 0 to 2 with an average value of 1. This value matches the hydrogen bond count of the cocrystal ligand AZD3839 and thus, imparts in the stability of the complex. The trajectory tracing hydrogen bond number is illustrated in Figure 10(d).

The implementation of isothermal-isobaric ensembles results in thermodynamic parameters like Van der Waals energy, electrostatic, polar solvation, solvent accessible surface area (SASA), and binding free energy. MM-PBSA of binding free energy of BACE1 & AZD3839 and BACE1 & Clitorin complexes were computed by MD simulation and the computed values are mentioned in Table 3. The high values of Van der Waals energy (-198.863 kJ/mol) were computed for the Clitorin complexed with BACE1. The high value of Van der Waals energy shows the high binding ability of the ligand to the binding site. The computed SASA values indicate the availability of sufficient surface area for the ligand attack that enables the ligand to bind properly to the protein. The low values of SASA for both BACE1 & AZD3839 (-19.633 kJ/mol) and BACE1 & Clitorin complex (-19.110 kJ/mol) are low enough to justify the better complexation of ligand to the protein. The value of polar solvation energy for BACE1 & AZD3839 (92.651 kJ/mol) is higher than the same for BACE1 & Clitorin complex (58.163 kJ/mol). This shows the availability of short-range dispersion interactions that are responsible for the formation of the cavity inside the macromolecule where the ligand binds. The binding free energy of the BACE1 & Clitorin (-164.643 kJ/mol) complex was higher than the BACE1 & AZD3839 (-155.552 kJ/mol). This shows the better binding of the protein-ligand complex than the cocrystal ligand and BACE1 complex.

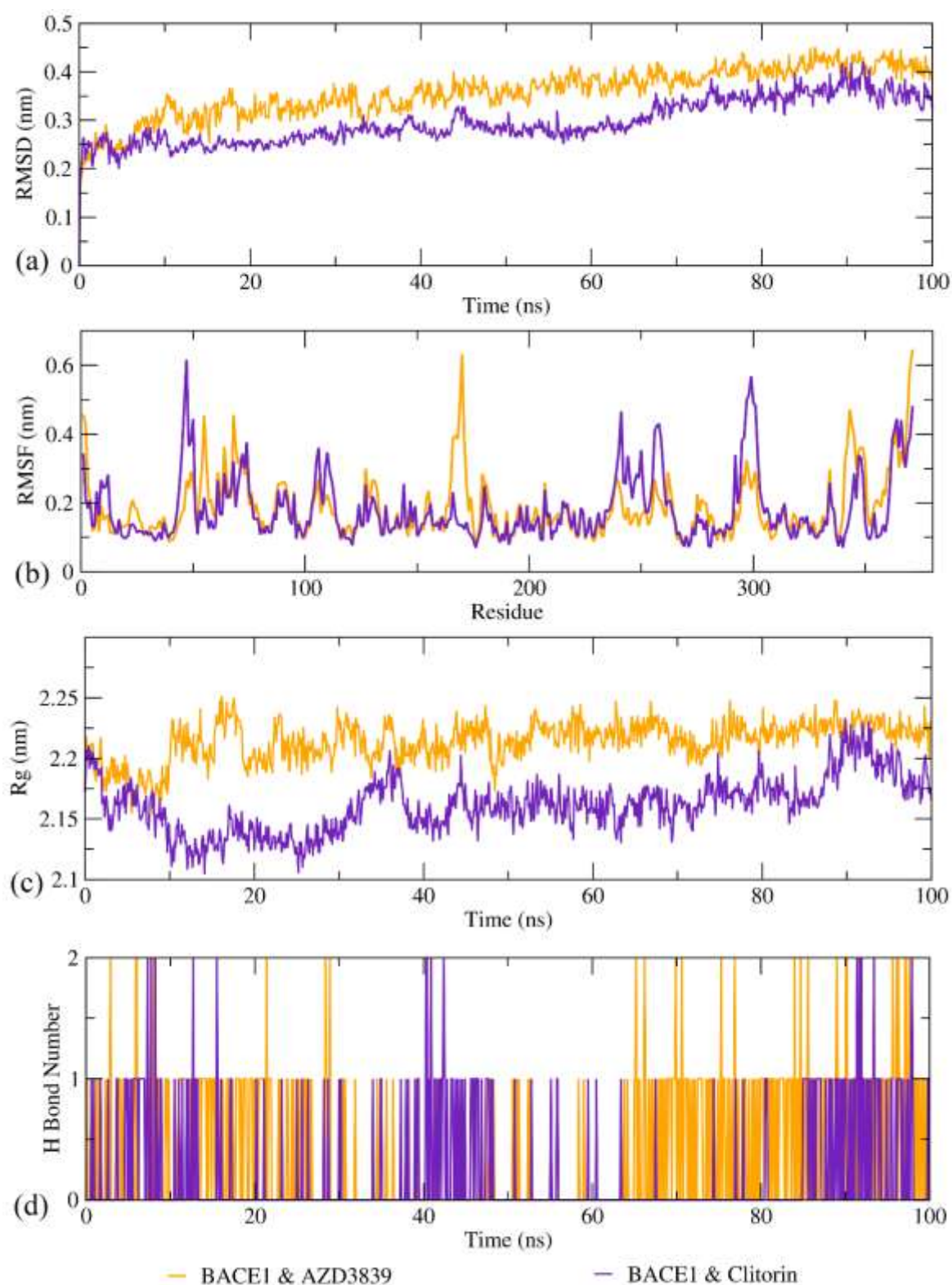


Figure 10. Trajectory analysis of molecular dynamics simulation of β -Site amyloid precursor protein cleaving enzyme1 (BACE1) with Clitorin and cocrystal ligand AZD3839 (PDB ID: 4B05) (a) RMSD of BACE1 & AZD3839 and BACE1 & Clitorin complexes (b) RMS fluctuation (c) R_g values and (d) Hydrogen bonds number between enzyme and ligands during the period of 100 ns simulation.

Table 3. MM-PBSA calculations of binding free energy of BACE1 & AZD3839 and BACE1 & Clitorin complexes between 80 ns and 100 ns.

| Parameters (Energy, kJ/mol) | Enzyme-ligand complexes | |
|---------------------------------------|--------------------------------|------------------|
| | BACE1 & AZD3839 | BACE1 & Clitorin |
| Van der Waals | -207.920±11.624 | -198.863±11.039 |
| Electrostatic | -20.750±5.466 | -4.834±10.773 |
| Polar solvation | 92.651±15.077 | 58.163±19.970 |
| SASA | -19.633±0.804 | -19.110±1.290 |
| Binding free | -155.652±13.441 | -164.643±13.762 |

3.6.3. Protein-ligand interactions from MD simulation

The position of the ligand bonded to the macromolecule at 0 ns (position after docking) and 100 ns was monitored and the position of the ligand bonded to protein at 0 ns and 100 ns of MD simulation is illustrated in Figure 11. The amino acid residues involved in interactions like Vander Waal's, pi-anion, pi-donor, pi-alkyl, and pi-stacked interactions of the protein-ligand complex at 0 ns, 50 ns, and 100 ns of the MD simulation are also analyzed to justify the variation in protein-ligand interactions. A gradual rise in the number of residues involved in the binding is observed during the simulation. The two-dimensional representation of residues involved in the interactions is shown in Figure 12. At 0 ns of the simulation, only Phe107, Asp32, Trp75, and Ile117 residues impart in forming pi-pi, pi-anion, pi-donor hydrogen bond, and pi-alkyl hydrophobic interactions (Figure 12(a)). Except for Trp75 which forms the hydrogen bond, the rest of the residues form hydrophobic interactions that are non-polar in nature. The number of residues increased at the 50 ns of simulation. Ala39, Tyr71, Val69, Ala99 and Leu79 (Figure 12(b)) were seemed to be associated with forming pi-sigma, pi-pi, and pi-stacked bonds. Thus, all the interactions at 50 ns were hydrophobic and hence non-polar in nature. The residue count at 100 ns was increased to 15 residues shown in green color in Figure 12(c) and they participate in the Vander Waals interactions. Ala39, Arg127, Ala99, and Leu79 residues make the pi-alkyl interactions and Tyr71 makes up the pi-pi stacked bonds. One pi-sigma interaction with the involvement of Val69 was also seen at 100 ns of the simulation time. Thus, the major part of the interactions at 100 ns is Vander Waal interactions that are polar. Thus, there is a change in interacting residues at 0 ns, 50 ns, and 100 ns of the simulation as well as in the chemical polarity of the complex.

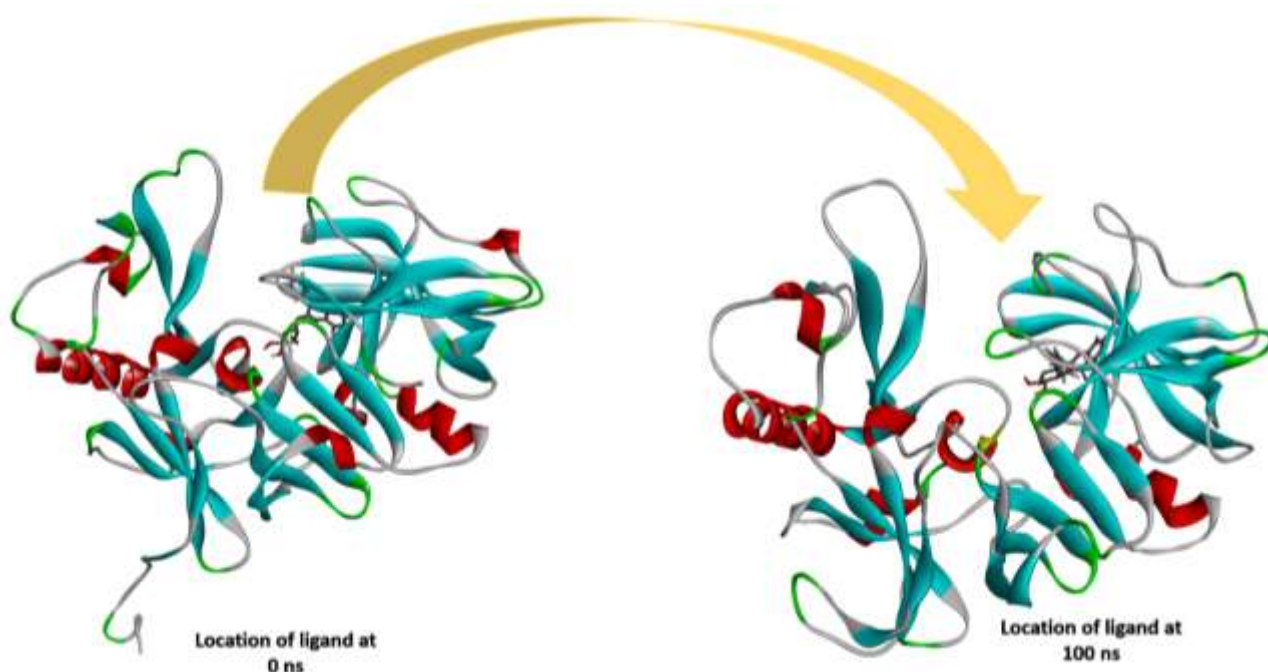


Figure 11. Diagram showing position of the ligand bonded to protein at 0 ns and 100 ns of MD simulation.

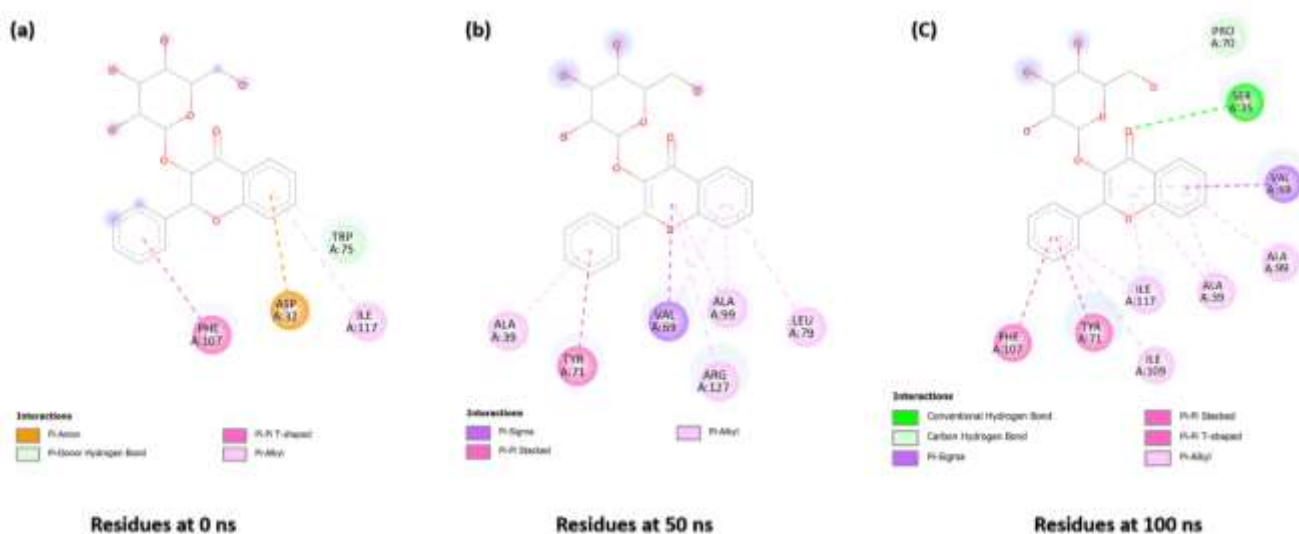


Figure 12. The 2D representation of amino acid residues involved in Vander Waal's, pi-anion, pi-donor, pi-alkyl, and pi-stacked interactions of the protein-ligand complex at (a) 0 ns, (b) 50 ns, and (c) 100 ns of the MD simulation. The specific type of interaction is indicated by a single color that is labeled at the bottom of the image.

3.6.4. Cardiac toxicity analysis

The probability map of Clitorin illustrated in Figure 13 indicates that –OH group is covered from the pink color. This pink-colored region shows that –OH part of the molecule imparts in the decrement of hERG blockage region. The confidence value for the Clitorin is 0.2 which doesn't exceed the limit. Thus, the probability map justifies that the Clitorin is an active potent against cardiotoxicity with 60% confidence value.

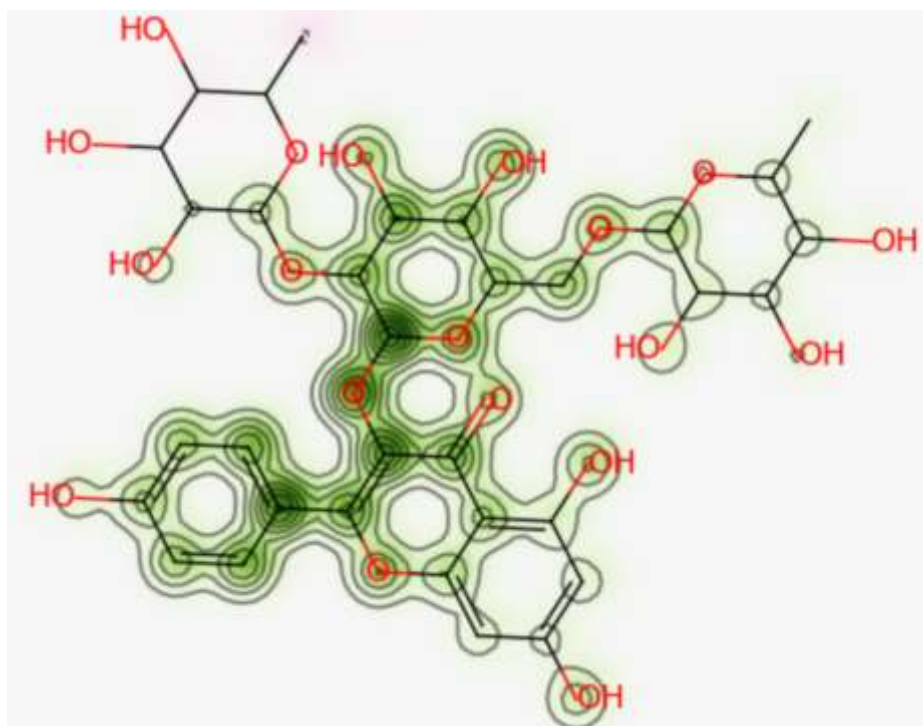


Figure 13. Probability map of Clitorin showing hERG blockage promoting regions in pink shade.

4. Conclusion

This study deals with the identification of a new organic NLO material, Clitorin, that is a phytochemical of *Clitoria ternatea* plant. The computational investigation done for the identification of novel characteristics of NLO material of Clitorin better reveals the target properties. The widespread nucleophilic and electrophilic regions of the MEP surface and charge variation in –OH groups, C – C bonds, and C = C bonds validate the availability of ICT in Clitorin. The spectral features like high Raman intensity and high wavelength for the electronic transitions were also observed for Clitorin. These factors better validate the dislocation of charge from the –OH groups towards the C – C bonds and C = C bonds of benzene rings. Thus, these parameters reveal the high reactivity of Clitorin. High reactivity induces the high magnitudes of α and β parameters. High reactivity, although, was seemed

during the docking and simulation also. Having the best binding affinity, and highest number of hydrogen bond interactions, Clitorin binds with the BACE1 target macromolecule of AD. The SASA values reveal the availability of a high interacting surface of protein towards the ligand. This leads to the high Vander Waal's interactions energy. The Vander Waal's interactions energy justifies the high chemical stability of the complex formed from docking. Thus, this study introduces a chemically reactive compound Clitorin that has NLO responses high enough to be used for experimental validations. Concurrently, it has high inhibiting potentiality against the BACE1 receptor of AD that gives rise to pathogens of AD in humans. Thus, it can be considered for clinical trials as an inhibitor against AD in the future.

Availability of data and material

Phytochemicals structure: <https://cb.imsc.res.in/imppat/home>

Extension conversion: http://openbabel.org/wiki/Main_Page

Optimization: <https://gaussian.com/>

Data analysis: <https://gaussian.com/gaussview6/>

Graph plotting: <https://www.originlab.com/>

Protein structure: <https://www.rcsb.org/>

Molecular docking: <https://vina.scripps.edu/>

Docking analysis: <https://discover.3ds.com/discovery-studio-visualizer-download>

MD Simulation: <https://www.gromacs.org/>

Cardiotoxicity analysis: <http://predherg.labmol.com.br/>

Acknowledges

Special thanks to WEBGRO Macromolecular Simulations (<https://simlab.uams.edu/index.php>) providing high-performance computing for their molecular dynamics simulations.

Author's Information

**1. Department of Physics, School of Sciences, Uttarakhand Open University,
Haldwani, 263139, Uttarakhand, India**

Shradha Lakhera, Meenakshi Rana & Kamal Devlal

**2. Department of Pharmaceutical Chemistry, Faculty of Pharmacy, Erciyes University,
Kayseri, 38039, Turkey**

Ismail Celik

Author's contribution

Authors: Shradha Lakhera, Kamal Devlal, Meenakshi Rana, Ismail Celik

Shradha Lakhera: Data curation, Writing-Original draft preparation, Visualization, Investigation, Software, Validation.

Kamal Devlal: Conceptualization, Writing- Reviewing and Editing

Meenakshi Rana: Conceptualization, Methodology, Writing-Reviewing and Editing, Supervision

Ismail Celik: Software handling, Reviewing and Editing

Correspondng author

Correspondance to Dr. Meenakshi rana

Conflict of interest:

The work: “Study of Nonlinear Optical Responses of Phytochemicals of *Clitoria ternatea* by Quantum Mechanical Approach and Investigation of their anti-Alzheimer activity with *In-Silico* Approach” by Shradha Lakhera, Dr. Kamal Devlal, Ismail Celik and myself is original research work done by the authors and have been submitted for publication in your esteemed journal “Structural chemistry” as an article. The authors declare that they have no known competing financial interests or personal relationships that could have appeared to influence the work reported in this paper.

References

- [1] C. R. Pye, M. J. Bertin, R. S. Lokey, W. H. Gerwick, R. G. Linington, Retrospective natural products analysis, *PNAS*. 2017, 114, 22, 5601-5606. <https://doi.org/10.1073/pnas.1614680114>
- [2] Z. A. Althman, M. M. Alam, M. Naushad, B. Alam, M. F. Khan. Inorganic Nanoparticles and Nanomaterials Based on Titanium (Ti): Applications in Medicine. *MSF*, 2013, 754 21–87. <https://doi.org/10.4028/www.scientific.net/msf.754.21>
- [3] M. Rana, N. Singla, A. Chatterjee, A. Shukla, P. Chowdhury, Investigation of nonlinear optical (NLO) properties by charge transfer contributions of amine functionalized tetraphenylethylene, *Opt. Mater.* 2016, 62, 80-89. <https://doi.org/10.1016/j.optmat.2016.09.043>
- [4] A. Buriahi, M. S. Singh, V. P. Arslan, Gamma-ray attenuation properties of some NLO materials: potential use in dosimetry. *Radiat Environ Biophys*. 2020, 59, 145–150. <https://doi.org/10.1007/s00411-019-00824-y>
- [5] L. Moroz, A. Maslovskaya, Fractional differential model of domain boundary kinetics in ferroelectrics: A computational approach, *AIP Conf Proc.* 2021, 2328, 020001. <https://doi.org/10.1063/5.0042140>
- [6] A. Sethi, R. Prakash, Novel synthetic ester of Brassicasterol, DFT investigation including NBO, NLO response, reactivity descriptor and its intramolecular interactions analyzed by AIM theory, *J. Mol. Struct.* 2015, 1083, 72-81. <https://doi.org/10.1016/j.molstruc.2014.11.028>
- [7] P. Khandel, S. K. Shahi, D. K. Soni, R. K. Yadaw. L. Kanwar, *Alpinia calcarata*: potential source for the fabrication of bioactive silver nanoparticles. *Nano Convergence*. 2018, 5, 37. <https://doi.org/10.1186/s40580-018-0167-9>
- [8] S. Pugazhendhi, R. Usha, F. Mary Anjalin, Comparative study of different plant extract mediated silver nanoparticles for nonlinear optics, *Mater. Today: Proc.* 2020, 33, 7, 3984-3988. <https://doi.org/10.1016/j.matpr.2020.06.336>
- [9] K. O. Falade, T. O. Olurin, E. A. Ike, O. C. Aworh, Effect of pretreatment and temperature on air-drying of *Dioscorea alata* and *Dioscorea rotundata* slices, *J. Food Eng.* 2007, 80, 4, 1002-1010. <https://doi.org/10.1016/j.jfoodeng.2006.06.034>
- [10] S. Jeyaram, T. Geethakrishnan, Spectral and third-order nonlinear optical characteristics of natural pigment extracted from *coriandrum sativum*, *Opt. Mater.* 2020, 107, 110148. <https://doi.org/10.1016/j.optmat.2020.110148>
- [11] S. Jeyaram, T. Geethakrishnan, Linear and nonlinear optical properties of chlorophyll-a extracted from *Andrographis paniculata* leaves, *Opt Laser Technol.* 2019, 116, 31-36. <https://doi.org/10.1016/j.optlastec.2019.03.013>
- [12] S. N. Margar, N. Sekar, Nonlinear optical properties of curcumin: solvatochromism-based approach and computational study, *Mol. Phys.* 2016, 114, 12, 1867-1879. <https://doi.org/10.1080/00268976.2016.1161248>

- [13] B. G. S. M. Sumanasinghe, R. N. Acharya, M. Nariya, K. Nishteswar, Pharmacological evaluation of vrishyakarma (Aphrodisiac activity) of leaf of *Clitoria ternatea* Linn. (Aparajita-Blue variety) *Int. J. Herb. Med.* 2020, 8, 3, 130-133.
- [14] N. A. Anuar, F. Pa'ee, N. A. Manan, N. A. M. Salleh, Effect of water stress on antibacterial activity, Total Phenolic Content and Total Flavonoid Content of *Clitoria ternatea*, *IOP Conf. Ser.: Earth Environ. Sci.* 2008, 736, 012008. <https://doi.org/10.1088/1755-1315/736/1/012008>
- [15] A. P. Nugraha, D. Rahmadhani, M. S. Puspitaningrum, Y. Rizqianti, V. D. Kharisma, D. S. Ernawati, Molecular docking of anthocyanins and ternatin in *Clitoria ternatea* as coronavirus disease oral manifestation therapy. *J Adv Pharm Technol Res.* 2021, 12, 4, 362-367. https://doi.org/10.4103/japtr.japtr_126_21
- [16] Ullah, A., Prottoy, N.I., Araf, Y., Hossain, S., Sarkar, B., and Saha, A. Molecular Docking and Pharmacological Property Analysis of Phytochemicals from *Clitoria ternatea* as Potent Inhibitors of Cell Cycle Checkpoint Proteins in the Cyclin/CDK Pathway in Cancer Cells. *Comput. Mol. Biosci.* 2019, 9, 81-94. <https://doi.org/10.4236/cmb.2019.93007>
- [17] S. Lakhera, K. Devlal, A. Ghosh, M. Rana, In Silico Investigation of Phytoconstituents of Medicinal Herb Piper Longum Against SARS-CoV-2 by Molecular Docking and Molecular Dynamics Analysis, Results in Chemistry. 2021, 100199. <https://doi.org/10.1016/j.rechem.2021.100199>
- [18] S. Lakhera, K. Devlal, A. Ghosh, M. Rana, Modelling the DFT structural and reactivity study of feverfew and evaluation of its potential antiviral activity against COVID-19 using molecular docking and MD simulations. *Chem. Pap.* 2022. <https://doi.org/10.1007/s11696-022-02067-6>
- [19] S. Lakhera, M. Rana, K. Devlal, I. Celik, R. Yadav, A comprehensive exploration of pharmacological properties, bioactivities and inhibitory potentiality of luteolin from *Tridax procumbens* as anticancer drug by in-silico approach, *Struct Chem.* 2022. <https://doi.org/10.1007/s11224-022-01882-7>
- [20] S. Sivanandhan, G. Pathalam, S. Antony, G. P. Michael, K. Balakrishna, A. Boovaragamurthy, O. Shiota, M. S. Alwahibi, M. S. El-Shikh, S. Ignacimuthu, Effect of monoterpene ester from *Blumea axillaris* (Lam.) DC and its acetyl derivative against plant pathogenic fungi and their in silico molecular docking, *Nat. Prod. Res.* 2021, 35, 24, 5744-5751. <https://doi.org/10.1080/14786419.2020.1833197>
- [21] K. Georgousaki, N. Tsafantakis, S. Gumeni, G. Lambrinidis, V. G. Menéndez, J. R. Tormo, O. Genilloud, I. P. Trougakos, N. Fokialakis, Biological Evaluation and In Silico Study of Benzoic Acid Derivatives from *Bjerkandera adusta* Targeting Proteostasis Network Modules, *Molecules.* 2020, 25, 3, 666. <https://doi.org/10.3390/molecules25030666>
- [22] Y. Bare, L. I. N. Indahsari, D. R. T. Sari, T. Watuguly, In Silico Study: Potential Prediction of *Curcuma longa* And *Cymbopogon citratus* Essential Oil As Lipoxxygenase Inhibitor, *JSMARTech.* 2021, 2, 2. <https://doi.org/10.21776/ub.jsmartech.2021.002.02.75>

- [23] K. N. Jiji, P. Muralidharan, Neuropharmacological Potential of *Clitoria ternatea* Linn. - A Review, *Research J. Pharm. and Tech.* 2020, 13, 11, 5497-5502. <https://doi.org/10.5958/0974-360X.2020.00960.9>
- [24] J. B. Morris, Multivariate Analysis of Butterfly Pea (*Clitoria ternatea* L.) Genotypes with Potentially Healthy Nutraceuticals and Uses, *Journal of Dietary Supplements*. 2022. <https://doi.org/10.1080/19390211.2021.2022821>
- [25] T. Fitrilia, M. F. Kurniawan, F. R. Kurniawati, T. Setiawan, The POTENTIAL OF BUTTERFLY PEA FLOWER METHANOL EXTRACT AS AN ANTIOXIDANT BY IN SILICO, *IJAR*. 2020, 1, 3, 163-169. <https://doi.org/10.30997/ijar.v1i3.64>
- [26] B. Anthika, S. P. Kusumocahyo, H. Sutanto, Ultrasonic Approach in *Clitoria ternatea* (Butterfly Pea) Extraction in Water and Extract Sterilization by Ultrafiltration for Eye Drop Active Ingredient, *Procedia Chem.* 2015, 16, 237-244. <https://doi.org/10.1016/j.proche.2015.12.046>.
- [27] P. Kosai, K. Sirisidhi, K. Jiraungkoorskul, W. Jiraungkoorskul, Review on Ethnomedicinal uses of Memory Boosting Herb, Butterfly Pea, *Clitoria ternatea*. *J. Nat. Remedies*. 2015, 71-76. <https://doi.org/10.18311/jnr/2015/480>
- [28] A. A. Margret, T. N. Begum, S. Parthasarathy, S. Suvaithenamudhan, Strategy to Employ *Clitoria ternatea* as a Prospective Brain Drug Confronting Monoamine Oxidase (MAO) Against Neurodegenerative Diseases and Depression, *Nat. Prod. Bioprospect.* 2015, 5, 293–306. <https://doi.org/10.1007/s13659-015-0079-x>
- [29] M. J. Frisch, G. W. Trucks, H. B. Schlegel, et al, Gaussian 09, Revision B. 01, Gaussian Inc., Wallingford CT, 2009, 121, 150-166.
- [30] A. D. Becke, Density-functional thermochemistry. III. The role of exact exchange, *J. Chem. Phys.* 98 5648. <https://doi.org/10.1063/1.464913>
- [31] A. D. Becke, Density-functional thermochemistry. V. Systematic optimization of exchange-correlation functionals, *J. Chem. Phys.* 1997, 107, 8554–8560. <https://doi.org/10.1063/1.475007>
- [32] T. Koopmans, Ordering of wave functions and eigen energies to the individual electrons of an atom. *Physica*. 1933, 1, 104–113. [https://doi.org/10.1016/S0031-8914\(34\)90011-2](https://doi.org/10.1016/S0031-8914(34)90011-2)
- [33] L. Zuo, B. T. Hemmelgarn, C. C. Chuang, T. M. Best, The Role of Oxidative Stress-Induced Epigenetic Alterations in Amyloid- β Production in Alzheimer's Disease, *Oxid Med Cell Longev.* 2015, 5, 604658. <https://doi.org/10.1155/2015/604658>
- [34] R. C. Braga, V. M. Alves, M. F. B. Silva, E. Muratov, D. Fourches, L. M. Liao, A. Tropsha, C. H. Andrade, Pred-hERG: A Novel web-Accessible Computational Tool for Predicting Cardiac Toxicity, *Mol Inform.* 2015, 34, 698-701. <https://doi.org/10.1002/minf.201500040>
- [35] H. Bekker, H.J.C. Berendsen, E.J. Dijkstra, S. Achterop, R. van Drunen, D. van der Spoel, A. Sijbers, H. Keegstra, "Gromacs: A parallel computer for molecular dynamics simulations", *Physics computing*. Edited by R.A. de Groot and J. Nadrchal. World Scientific, Singapore. 1993, 92, 252–256.

- [36] M. J. Abraham, T. Murtola, R. Schulz, S. Páll, J.C. Smith, B. Hess, E. Lindahl, "GROMACS: High performance molecular simulations through multi-level parallelism from laptops to supercomputers," *SoftwareX*. 2015, 1, 19–25. <https://doi.org/10.1016/j.softx.2015.06.001>
- [37] Q. Cheng, X. Shi, C. Li, Y. Jiang, Z. Shi, J. Zou, X. Wang, X. Wang, Z. Cui, Chromophores with side isolate groups and applications in improving the poling efficiency of second non-linear optical (NLO) materials, *Dyes and Pigments*. 2019, 162, 721-727. <https://doi.org/10.1016/j.dyepig.2018.11.001>.
- [38] S. T. Lee, W. M. Khairul, O. J. Lee, R. Rahamathullah, A. I. Daud, K. Halim, K. Bulat, S. Sapari, F. I. A. Razak, G. Krishnan, Electronic, reactivity and third order nonlinear optical properties of thermally-stable push-pull chalcones for optoelectronic interest: Experimental and DFT assessments, *Journal of Physics and Chemistry of Solids*. 2021, 159, 110276. <https://doi.org/10.1016/j.jpcs.2021.110276>
- [39] A. Ozarslan, D. Çakmaz, F. Erol, H. Şenöz, N. Seferoğlu, A. Barsella, Z. Seferoğlu, Synthesis and investigation of photophysical, NLO and thermal properties of D- π -A- π -D dyes. 2020, 129583. <https://doi.org/10.1016/j.molstruc.2020.129583>
- [40] I. M. Pavlovetc, S. Draguta, M. I. Fokina, T. V. Timofeeva, I. Y. Denisyuk, Synthesis, crystal growth, thermal and spectroscopic studies of acentric materials constructed from aminopyridines and 4-nitrophenol, *Opt. Commun.* 2016, 362, 64-68. <https://doi.org/10.1016/j.optcom.2015.05.034>
- [41] V. Krishnakumar, R. Nagalakshmi, Studies on the first-order hyperpolarizability and terahertz generation in 3-nitroaniline, *Physica B: Condensed Matter*, 2008, 403, 10, 1863-1869. <https://doi.org/10.1016/j.physb.2007.10.341>
- [42] D. Marappan, M. Palanisamy, H. Mon-Shu, B. Balraj, C Sivakumar, Growth, Vibrational, Optical, Mechanical and DFT Investigations of an Organic Nonlinear Optical Material – Phenylurea" *Zeitschrift für Physikalische Chemie*, 2019, 233, 11, 1659-1682. <https://doi.org/10.1515/zpch-2018-1230>
- [43] R. Jawaria, M. Hussain, M. Khalid, M. U. Khan, M. N. Tahir, M. M. Naseer, A. A. C. Braga, Z. Shafiq, Synthesis, crystal structure analysis, spectral characterization and nonlinear optical exploration of potent thiosemicarbazones based compounds: A DFT refine experimental study, *Inorg. Chim. Acta*, 2019, 486, 162-171. <https://doi.org/10.1016/j.ica.2018.10.035>
- [44] R. Thirumurugan, B. Babu, K. Anitha, J. Chandrasekaran, Synthesis, growth, characterization and quantum chemical investigations of a promising organic nonlinear optical material: Thiourea-glutaric acid, *J. Mol. Struct.* 2018, 1171, 915-925. <https://doi.org/10.1016/j.molstruc.2017.07.027>
- [45] M. Rana, P. Chowdhury, Nonlinear optical responses of organic based indole derivative: An experimental and computational study, *Mater. Today: Proc.* 2020, 28, 241-245. <https://doi.org/10.1016/j.matpr.2020.01.598>

- [46] M. Faizan, M. Mehkoom, Z. Afroz, V. H. N. Rodrigues, S.M. Afzal, S. Ahmad, Experimental and computational investigation of novel dihydrated organic single crystal of 2,4,6-triaminopyrimidine and 3,5-dinitrobenzoic acid: Linear and nonlinear optical response with limiting performance, J. Solid State Chem. 2021, 300, 122255. <https://doi.org/10.1016/j.jssc.2021.122255>.
- [47] M. T. O. Abe, C. L. Nzia, L. S. Sidjui, et al. Predictive calculation of structural, nonlinear optical, electronic and thermodynamic properties of andirobin molecule from ab initio and DFT methods. SN Appl. Sci.2021, 3, 768. <https://doi.org/10.1007/s42452-021-04749-4>

Supplementary Files

This is a list of supplementary files associated with this preprint. Click to download.

- [Graphicalabstract.pdf](#)
- [ResearchHighlight.docx](#)
- [supportingdocument.docx](#)